Electronic Supplementary Information (ESI)
This journal is (c) The Royal Society of Chemistry 2022

Controllable sensitization of Zr-MOFs by CdS and its application for photoelectrochemical detection of alkaline phosphatase

Ying Ying, Wenying Wu, Guihua He, Wenfang Deng, Yueming Tan*, and Qingji Xie

Key Laboratory of Chemical Biology and Traditional Chinese Medicine Research (Ministry of Education of China), College of Chemistry and Chemical Engineering, Hunan Normal University, Changsha 410081, China

*E-mail: tanyueming0813@hunnu.edu.cn

Experimental section

Instrumentation. Transmission electron microscopy (TEM) studies were performed on a TECNAI F-30 high-resolution transmission electron microscope. Scanning electron microscopy (SEM) images were obtained with a JSM-6360 field emission scanning electron microscope. X-ray diffraction (XRD) pattern was obtained on a PANalytical X'pert Pro X-ray diffractometer using Cu Kα radiation, operating at 40 kV and 30 mA, with a scan rate of 4° min^{-1}. X-ray photoelectron spectroscopy (XPS) measurement was investigated using a Thermo Scientific K-Alpha Xray photoelectron spectroscopic instrument. Ultraviolet-visible diffused reflectance spectra were recorded on a UV-2006i spectrophotometer (Shimadzu, Japan). Fourier transform infrared (FT-IR) spectra were collected on Nicolet Nexus 670 Fourier transform infrared spectrometer. All electrochemical experiments were performed on a CHI760E electrochemical workstation. All photoelectrochemical experiments were carried out using a CEL-HXF300 xenon lamp light source system equipped with a monochromator (400-700 nm). The light intensity is 100 mW cm^{-2}.

Reagents. Cadmium chloride ($CdCl_2 \cdot 2.5H_2O$), Cadmium nitrate ($Cd(NO_3)_2 \cdot 4H_2O$), $Na_2S \cdot 9H_2O$, thioglycolic acid, citric acid, Zirconium chloride ($ZrCl_4$), terephthalic acid (H_2BDC), dimethylformamide (DMF), acetic acid, ethanol, sodium tripolyphosphate (STPP), magnesium chloride, zinc chloride, and Tris were purchased from Sinopharm Chemical Reagent Co. Ltd. (Shanghai, China). *N*-hydroxysuccinimide (NHS), carbodiimide hydrochloride (EDC·HCl), L-cysteine (L-cys), glucose oxidase (GOx), lysozyme and bovine serum albumin (BSA) were purchased from Sigma Aldrich. Alkaline phosphatase (ALP) and DNA were purchased from Sangon Biotech (Shanghai, China). Various concentrations of

ALP were obtained by diluting ALP with the Tris-HCl (0.01 M, pH 8.2) buffer containing 5 mM $MgCl_2$ and 0.1 mM $ZnCl_2$. All other reagents were of analytical grade and used without further purification. Milli-Q ultrapure water (Millipore, ≥18 MΩ cm) was used throughout.

Preparation of UiO-66. UiO-66 was synthesized following a reported method.[1] In brief, a solution was prepared by dissolving 598.6 mg of $ZrCl_4$, 425.6 mg of terephthalic acid, and 20 mL acetic acid in 60 mL DMF and stirred for 1 h. Then, the mixed solution was transferred to a 100 mL Teflon-lined autoclave and maintained at 120 ℃ for 24 h. After cooling, the final sample is obtained by centrifugation, washing and drying.

Preparation of CdS QDs. CdS QDs were synthesized following a reported method.[2] In brief, 250 μL of thioglycolic acid was added to 50 mL of 0.01 M $CdCl_2$ aqueous solution, and the pH value of the above solution was adjusted to 11 with 1.0 M NaOH aqueous solution. The solution was bubbled with N_2 for 30 min to remove dissolved oxygen in the solution. Then, 5.5 mL of 0.1 M Na_2S aqueous solution was injected into the solution, and the solution was refluxed under N_2 atmosphere for 4 h to obtain thioglycolic acid-capped CdS QDs. Finally, the solution was centrifuged, and the collected products were washed and dried in a 60 °C oven.

Preparation of CdS QDs-ssDNA. Thioglycolic acid-capped CdS QDs were conjugated with amino-terminated ssDNA through amide bonds. In brief, 1 mL of thioglycolic acid-capped CdS QDs (0.1 mg mL^{-1}) was dispersed in 1 mL of MES buffer (0.1 M, pH 6.0) containing 3 mg mL^{-1} NHS and 2 mg mL^{-1} EDC·HCl, and the resulting solution was gently shaken at room temperature for 60 min. Then the solution was centrifuged at 11,000 rpm for 10 min, and the collected products were washed with ultrapure water three times to remove excess EDC and

NHS. The activated CdS QDs were redispersed in 2 mL of ssDNA (5 μM), and the mixture was shaken overnight at room temperature. The obtained CdS QDs-ssDNA conjugates were redispersed in 2 mL of 10 mM Tris-HCl buffer (pH 7.4) and stored at 4 °C for later use.

Preparation of CdS NPs and CdS NPs-ssDNA. CdS nanoparticles (NPs) were synthesized following a reported method with slight modifications.[3] A solution was prepared by dissolving $Cd(NO_3)_2 \cdot 4H_2O$ (1.54 g) and citric acid (0.96 g) in water (50 mL). Then 50 mL of solution containing 5 mmol $Na_2S \cdot 9H_2O$ was dropped into the above solution, and the solution was stirred for 30 min. Subsequently, the prepared suspension was centrifuged, washed three times with deionized water and absolute ethanol, and dried in a 60 °C oven. The preparation of CdS NPs-ssDNA was similar to that of CdS QDs-ssDNA except that CdS NPs were used instead.

PEC detection of ALP activity. The UiO-66/ITO electrode was prepared by casting 20 μL of UiO-66 suspension (1 mg mL^{-1}) on clean ITO (electrode area: 0.25 cm^2). A series of solutions containing 2 mM STPP and different concentrations of ALP were prepared in the buffer (pH 8.2, 0.01 M Tris-HCl + 5 mM $MgCl_2$ + 0.1 mM $ZnCl_2$) and incubated at 37 °C for 20 min. Then the UiO-66/ITO electrode was incubated with the above solutions at 37 ℃ for 15 min. Subsequently, the photoelectrode was further incubated with the above CdS QDs-ssDNA suspension at 37 °C for 15 min. After each step, the electrode was rinsed with Tris-HCl buffer at least 3 times. Finally, the prepared electrode was used as the working electrode for PEC detection at 0 V under the visible light irradiation in a three-electrode system, with a platinum wire as the counter electrode and saturated calomel electrode as the reference electrode. 0.1 M

phosphate buffer solution (PBS, pH 7.4) containing 0.1 M ascorbic acid (AA) served as the electrolyte for PEC detection.

ALP activity detection in serum samples. The serum samples used in this experiment were provided by volunteers from the Fourth Hospital of Changsha City. Before use, they were centrifuged at 3000 rpm for 20 minutes to remove the precipitate in the serum. The supernatant was diluted 10 times, and ALP standard samples (0, 1.00, 2.00, and 5.00 U L^{-1}) were spiked. PEC detection of ALP activity in serum samples was similar to that in the buffer.

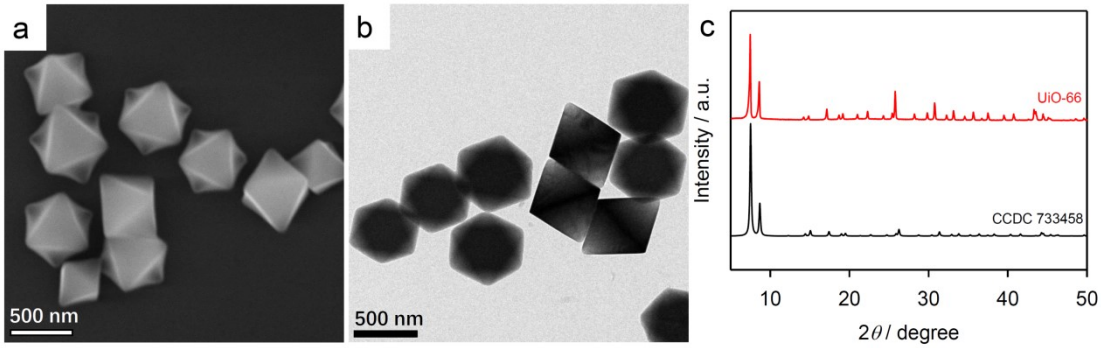

Fig. S1 (a) SEM image, (b) TEM image, and (c) XRD pattern of UiO-66 octahedras.

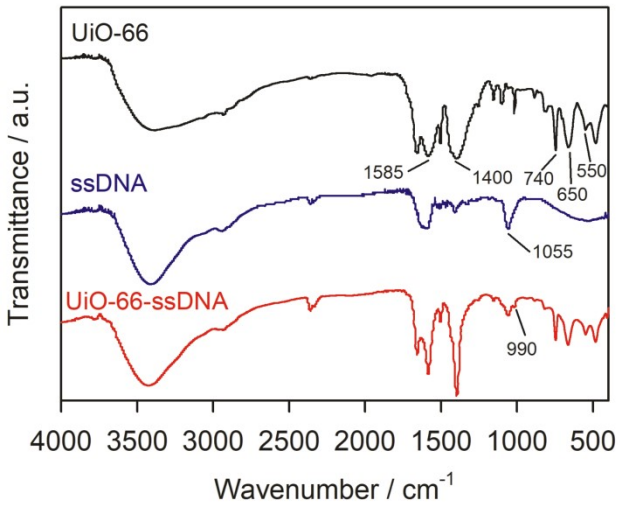

Fig. S2 FT-IR spectra of (a) UiO-66, (b) ssDNA, and (c) UiO-66-ssDNA conjugates.

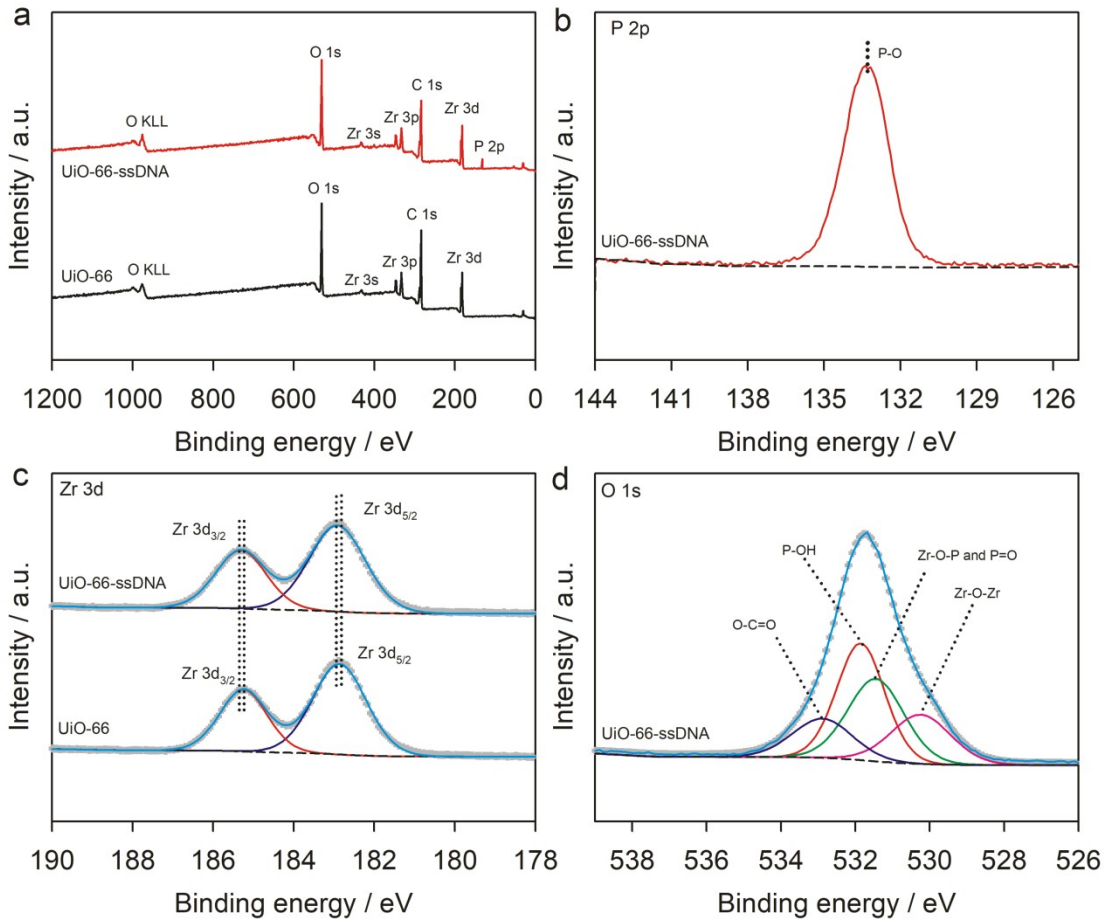

Fig. S3 (a) XPS survey spectra of UiO-66 and UiO-66-ssDNA conjugates. (b) High-resolution P 2p peak of UiO-66-ssDNA conjugates. (c) High-resolution Zr 3d peaks of UiO-66 and UiO-66-ssDNA conjugates. (d) High-resolution O 1s peak of UiO-66-ssDNA conjugates.

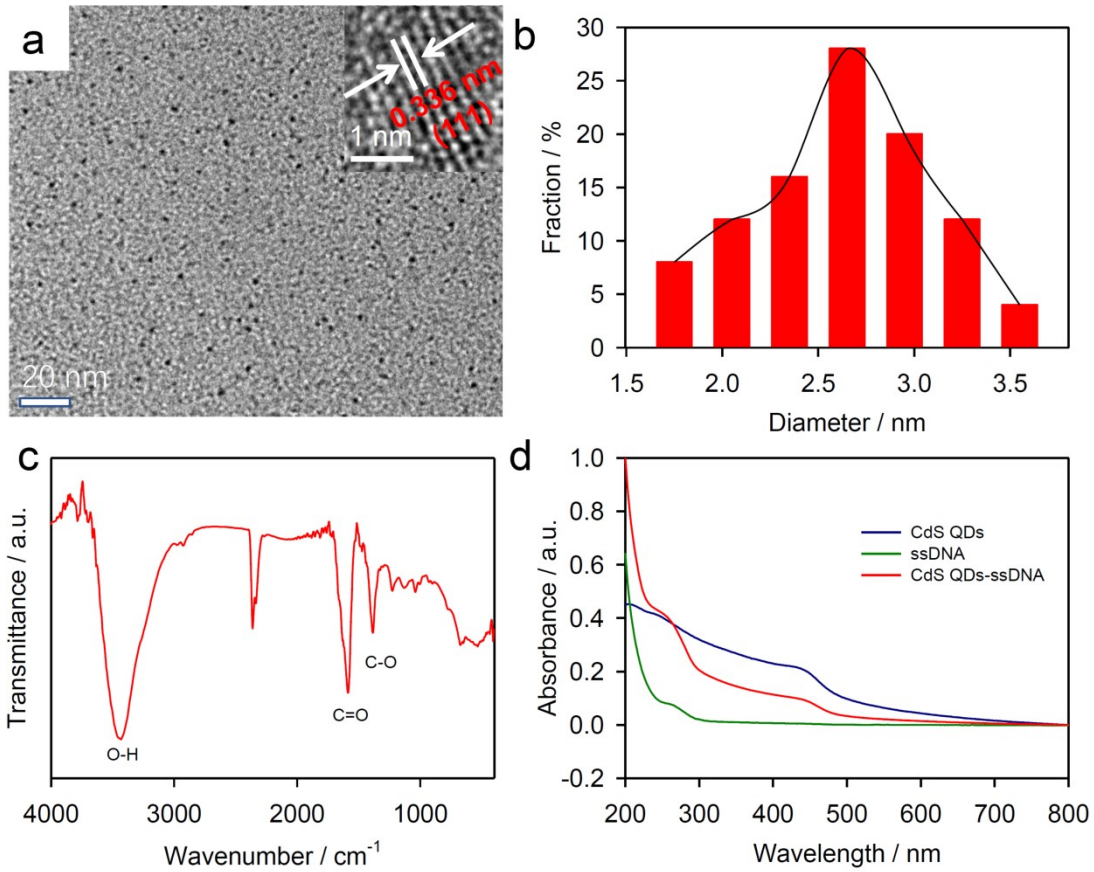

Fig. S4 (a) TEM image, (inset) HRTEM image, (b) size distribution, and (c) FT-IR spectrum of CdS QDs. (d) UV-vis absorption spectra of CdS QDs, ssDNA, and CdS QDs-ssDNA conjugates.

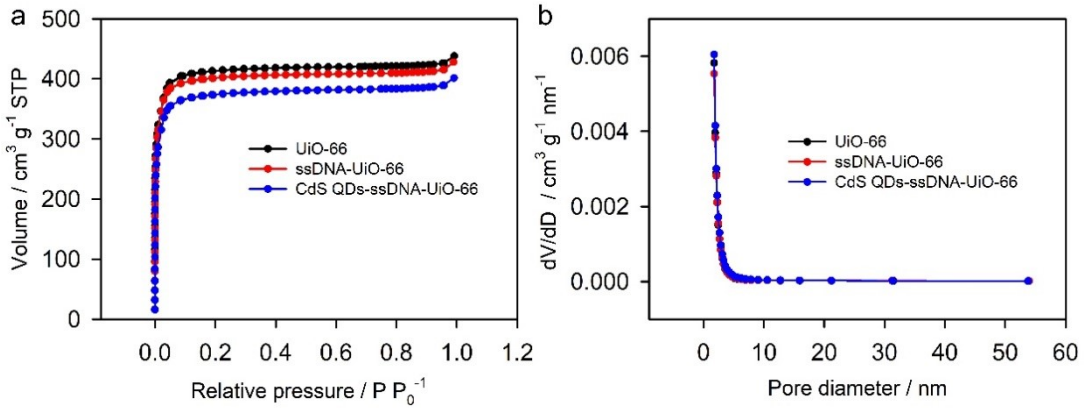

Fig. S5 (a) N_2 adsorption-desorption curves and (b) pore size distribution of UiO-66, ssDNA-UiO-66 and CdS QDs-ssDNA-UiO-66.

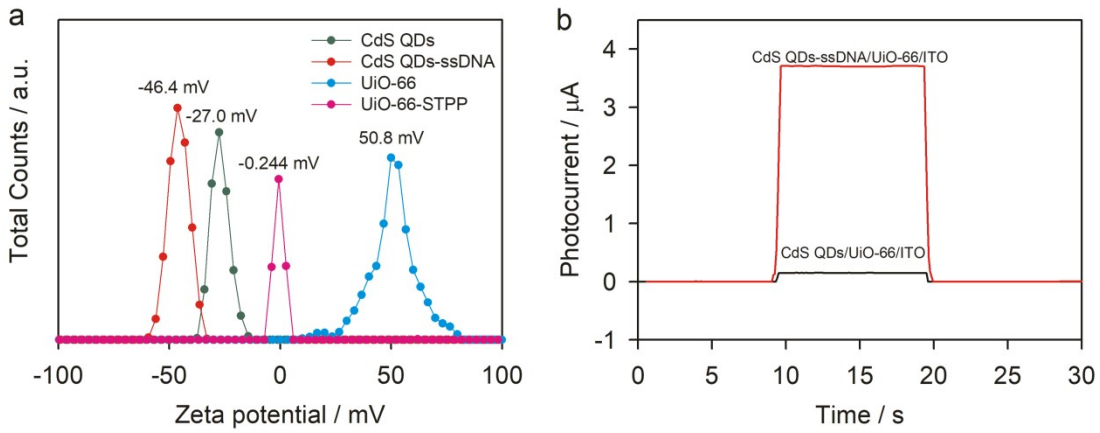

Fig. S6 (a) Apparent Zeta potential of CdS QDs, CdS QDs-ssDNA, UiO-66 and UiO-66-STPP. (b) Transient photocurrents of UiO-66/ITO after the incubation with CdS QDs and CdS QDs-ssDNA at 37 °C for 15 min.

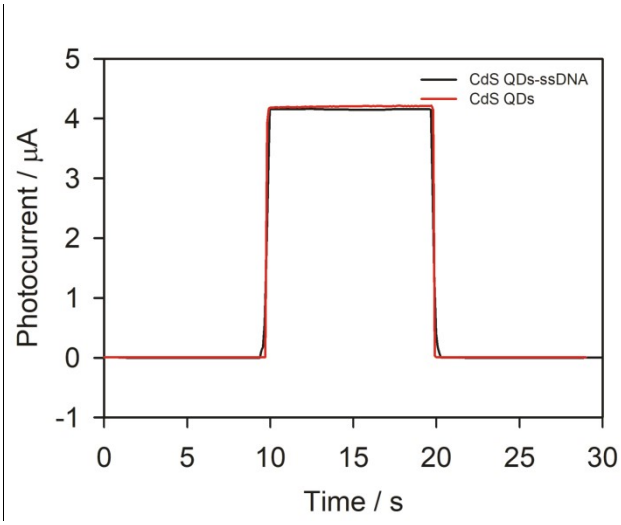

Fig. S7 Transient photocurrents of CdS QDs and CdS QDs-ssDNA casted directly on UiO-66/ITO.

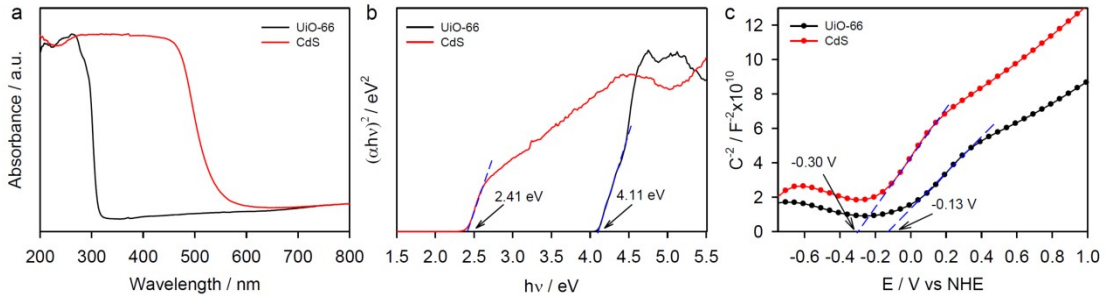

Fig. S8 (a) UV-vis diffuse reflectance spectra, (b) Plots of $(\alpha h\nu)^2$ vs hν, and (c) Mott-Schottky plots of UiO-66 and CdS QDs.

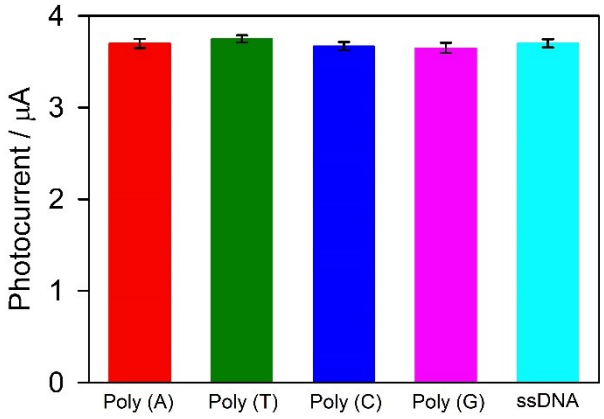

Fig. S9 Transient photocurrents of CdS QDs-Poly(A)/UiO-66/ITO, CdS QDs-Poly(T)/UiO-66/ITO, CdS QDs-Poly(C)/UiO-66/ITO, CdS QDs-Poly(G)/UiO-66/ITO and CdS QDs-ssDNA/UiO-66/ITO.

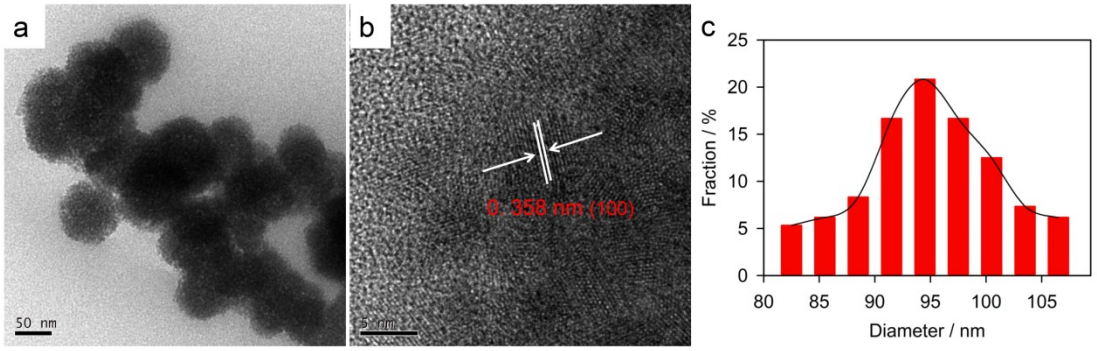

Fig. S10 (a) TEM image, (b) HRTEM image of CdS NPs and (c) size distribution CdS NPs.

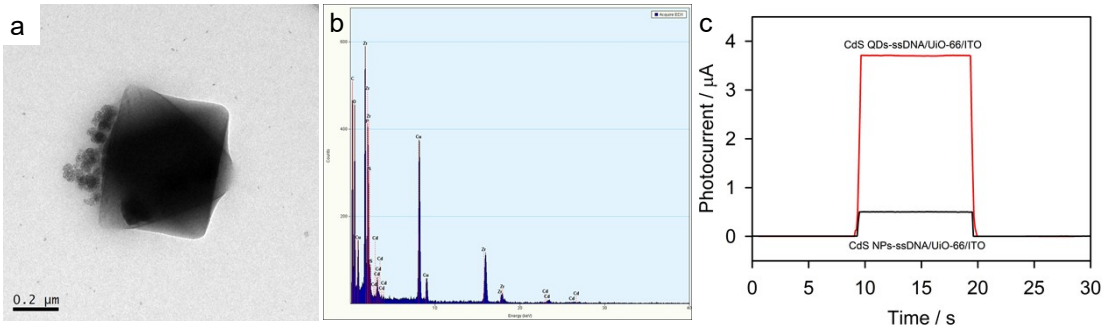

Fig. S11 (a) TEM, (b) EDX spectrum, and (c) transient photocurrents of CdS NPs-ssDNA/UiO-66.

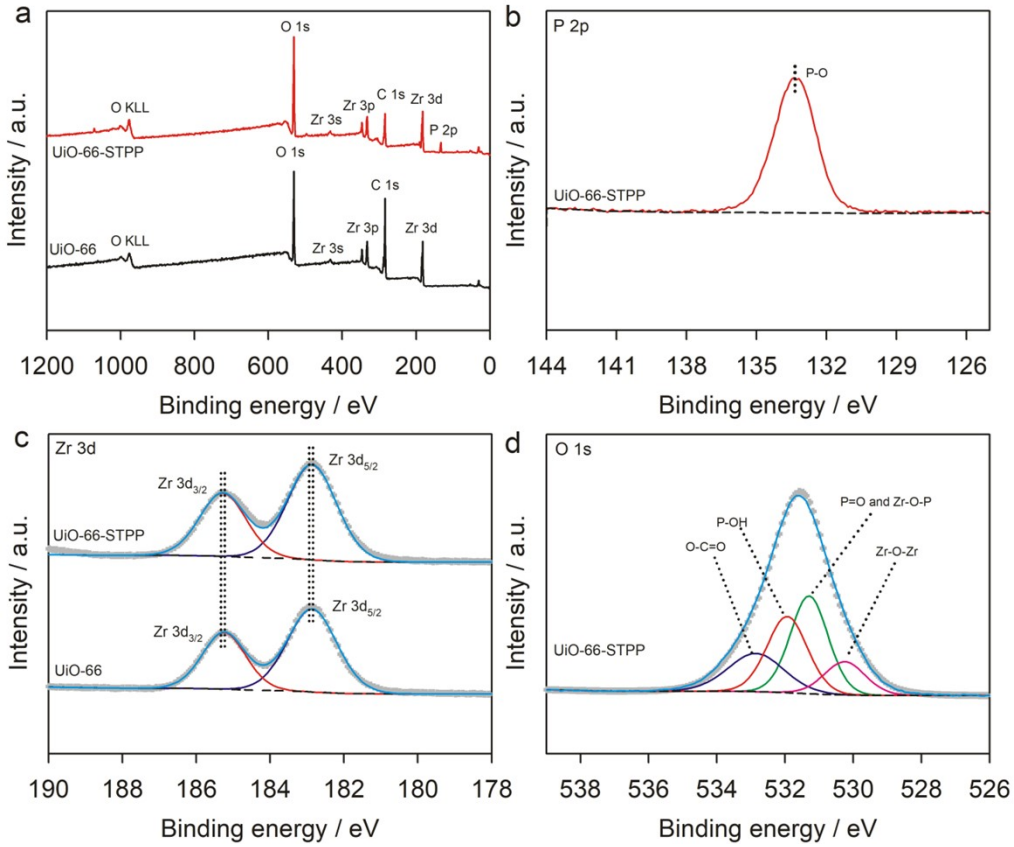

Fig. S12 (a) XPS survey spectra of UiO-66 and UiO-66-STPP conjugates. (b) High-resolution P 2p, (c) Zr 3d, and (d) O 1s peak of UiO-66-STPP conjugates.

In the XPS survey spectrum of UiO-66-STPP conjugates (**Fig. S12a**), P element is identified besides Zr, O and C, confirming that STPP is attached on UiO-66. The P 2p peak at 133.4 eV is assigned to P-O bonds (**Fig. S12b**). Due to the formation of Zr−O−P bonds, the binding energies of Zr $2d_{3/2}$ (185.3 eV) and Zr $2d_{5/2}$ (182.9 eV) for UiO-66-STPP conjugates show significant red shift, as compared to those for pristine UiO-66 (**Fig. S12c**). The O1s peak of UiO-66-STPP conjugates is deconvoluted into O−C=O at 533.0 eV, P−OH at 531.9 eV, Zr−O−P and P=O at 531.5 eV, and Zr−O−Zr at 530.2 eV (**Fig. S12d**). These results verify that STPP can be attached to UiO-66 through Zr−O−P bonds.

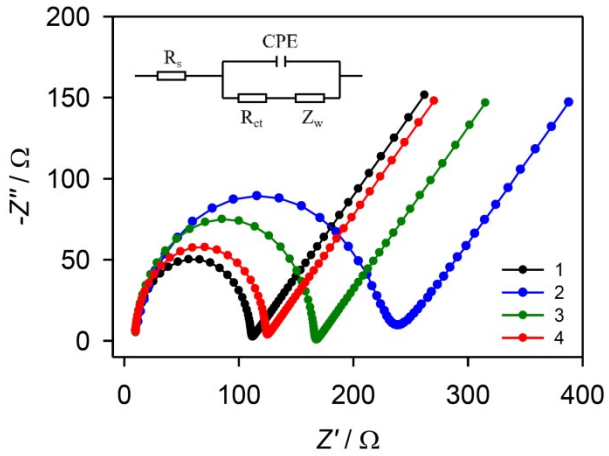

Fig. S13 Electrochemical impedance spectra of UiO-66/ITO after different incubations in 0.1 M aqueous KCl containing 5.0 mM $[Fe(CN)_6]^{3-/4-}$. (1) UiO-66/ITO, (2) UiO-66/ITO after incubation with 2 mM STPP, (3) UiO-66/ITO after incubation with 2 mM STPP and 0.1 U mL^{-1} ALP, and (4) UiO-66/ITO after incubation with 2 mM STPP and 1 U mL^{-1} ALP. The incubation time is 15 min. Inset shows Randles equivalent circuit model.

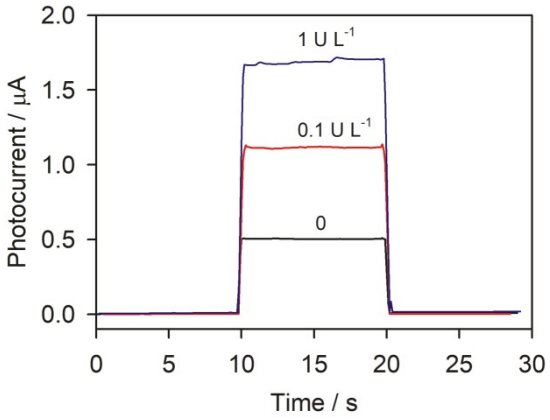

Fig. S14 Transient photocurrents of UiO-66/ITO after controllable sensitization with CdS QDs. The UiO-66/ITO was incubated with a mixture containing 2 mM STPP and ALP of different activities (0, 0.1, and 1 U L^{-1}), followed by the incubation with CdS QDs-ssDNA.

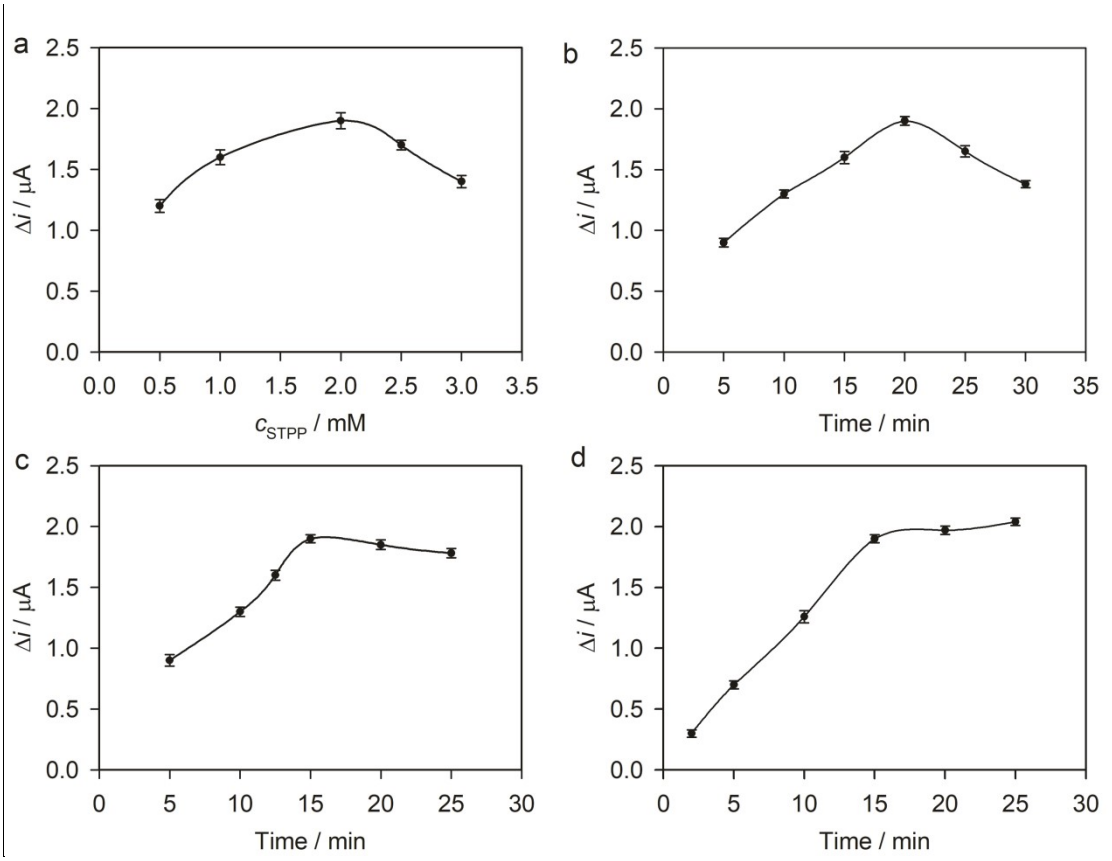

Fig. S15. Effects of (a) STPP concentration, (b) STPP hydrolysis time, (c) STPP attachment time, and (d) CdS QDs-ssDNA attachment time on photocurrent responses for detecting 10 U L^{-1} ALP.

To achieve the highest current response for the detection of ALP activity, some experimental parameters were optimized. The current response (Δi, μA) is defined as i-i_0, where i is the current for detecting a certain concentration of ALP, and i_0 is the current for the blank. Moderate site occupancy effect is conducive to obtaining a high Δi value. When the site occupancy effect is too strong, the value of i is too low, resulting in low Δi value; when the site occupancy effect is too weak, the value of i_0 is too high, also resulting in low Δi value. As shown in **Fig. S15a**, the Δi values increase with the increase of STPP concentration from 0.5 to 2.0 mM and then decrease with the increase of STPP concentration from 2.0 to 3.0 mM, because moderate STPP concentration can lead to moderate site occupancy effect. Hence, the optimum STPP concentration is 2 mM. STPP can be hydrolyzed by ALP, and

moderate STPP hydrolysis time can lead to moderate site occupancy effect. As a result, the STPP hydrolysis time is optimized to be 20 min (**Fig. S15b**). Similarly, the STPP attachment time is optimized to be 15 min (**Fig. S15c**), because moderate STPP attachment time can lead to moderate site occupancy effect. As shown in **Fig. S15d**, the Δi values increase with the increase of CdS QDs-ssDNA attachment time from 2 to 15 min, and then become almost unchanged, suggesting that the attachment of CdS QDs-ssDNA on UiO-66 has been basically completed in 15 min. Hence, the optimal time for CdS QDs-ssDNA attachment in this experiment is 15 min.

Table S1. The BET surface areas and pore diameters of UiO-66, ssDNA-UiO-66 and CdS QDs-ssDNA-UiO-66.

Sample	S_{BET} (m^2 g^{-1})	Average Pore Diameter (nm)
UiO-66	1223.31	2.10
ssDNA-UiO-66	1212.58	2.08
CdS QDs-ssDNA-UiO-66	1140.58	2.09

Table S2. Sequences of oligonucleotides used in this work

Name	Sequences from 5' to 3'
ssDNA	TACGACTCACTATAG-$(CH_2)_6$-NH_2
Poly(A)	AAAAAAAAAAAAAAA-$(CH_2)_6$-NH_2
Poly(T)	TTTTTTTTTTTTTTT-$(CH_2)_6$-NH_2
Poly(C)	CCCCCCCCCCCCCCC-$(CH_2)_6$-NH_2
Poly(G)	GGGGTGGGGTGGGGG-$(CH_2)_6$-NH_2

Table S3. The comparison of the determination of ALP in the literature.

Technique	Linear range ($U\ L^{-1}$)	Detection limit ($U\ L^{-1}$)	Ref.
Fluorescence	2.0-100.0	0.55	[4]
Fluorescence	30.0-240.0	5.00	[5]
Fluorescence	25.0-200.0	10.00	[6]
Fluorescence	0.5-100.0	0.19	[7]
Fluorescence	2.0-100.0	0.18	[8]
Electrochemical	0.1-100	0.02	[9]
Electrochemical	20-1500	3	[10]
Electrochemiluminescence	2.0-25.0	2	[11]
Electrochemiluminescence	0.1-6	0.037	[12]
Colorimetric	0.5-25	0.1	[13]
Photoelectrochemical	0.06-600	0.03	[14]
Photoelectrochemical	0.5-40	0.33	[15]
Photoelectrochemical	0.04-400	0.022	[16]
Photoelectrochemical	2.0-1500	1.7	[17]
Photoelectrochemical	10-300	1.5	[18]
Photoelectrochemical	0.01-500	0.005	This work

Table S4. Results of determination of ALP activity in a human serum sample.

Original (U L^{-1})	Added (U L^{-1})	Found (U L^{-1})	Recovery (%)	RSD (%)
	1.00	3.14	103	3.6
2.11	2.00	4.10	99.5	4.1
	5.00	7.04	98.6	7.7

References

1 J. H. Cavka, S. Jakobsen, U. Olsbye, N. Guillou, C. Lamberti, S. Bordiga and K. P. Lillerud, *J. Am. Chem. Soc.* 2008, **130**, 13850-13851.

2 W.-W. Zhao, R. Chen, P.-P. Dai, X.-L. Li, J.-J. Xu and H.-Y. Chen, *Anal. Chem.* 2014, **86**, 11513-11516.

3 F. Q. Zhou, J. C. Fan, Q. J. Xu and Y. L. Min, *Appl. Catal., B*, 2017, **201**, 77-83.

4 Y. Li, Z.-Z. Huang, Y. Weng and H. Tan, *Chem. Commun.* 2019, **55**, 11450-11453.

5 J.-L. Ma, B.-C. Yin, X. Wu and B.-C. Ye, *Anal. Chem.* 2016, **88**, 9219-9225.

6 M. Cai, C. Ding, F. Wang, M. Ye, C. Zhang and Y. Xian, *Biosens. Bioelectron.* 2019, **137**, 148-153.

7 K. Yu, T. Wei, Z. Li, J. Li, Z. Wang and Z. Dai, *J. Am. Chem. Soc.* 2020, **142**, 21267-21271.

8 C. Wang, G. Tang and H. Tan, *J. Mater. Chem. B* 2018, **6**, 7614-7620.

9 J. Peng, X.-X. Han, Q.-C. Zhang, H.-Q. Yao and Z.-N. Gao, *Anal. Chim. Acta* 2015, **878**, 87-94.

10 L. Sappia, B. Felice, M. A. Sanchez, M. Marti, R. Madrid and M. I. Pividori, *Sens. Actuators, B* 2019, **281**, 221-228.

11 H. Jiang and X. Wang, *Anal. Chem.* 2012, **84**, 6986-6993.

12 S. Li, J. Li, B. Geng, X. Yang, Z. Song, Z. Li, B. Ding, J. Zhang, W. Lin and M. Yan, *Microchem. J.* 2021, **164**, 106041.

13 H. Song, K. Ye, Y. Peng, L. Wang and X. Niu, *J. Mater. Chem. B* 2019, **7**, 5834-5841.

14 F. X. Wang, C. Ye, S. Mo, L. L. Liao, X. F. Zhang, Y. Ling, L. Lu, H. Q. Luo and N. B. Li, *Analyst* 2018, **143**, 3399-3407.

15 S. Jiao, L. Liu, J. Wang, K. Ma and J. Lv, *Small* 2020, **16**, 2001223.

16 C.-Q. Zhao, J. Zhou, K.-W. Wu, S.-N. Ding, J.-J. Xu and H.-Y. Chen, *Anal. Chem.* 2020, **92**, 6886-6892.

17 R. Yang, X. Yan, Y. Li, X. Zhang and J. Chen, *ACS Appl. Mater. Interfaces* 2017, **9**, 42482-42491.

18 W. Kong, Q. Tan, H. Guo, H. Sun, X. Qin and F. Qu, *Microchim. Acta* 2019, **186**, 73.